Radiofrequency transmission through rectangular apertures in perimetrally uncoated low emissivity windows

Rocio Chueca[1], Raul Alcain[1], Carlos Heras[1] and Iñigo Salinas[1]

[1]Grupo de Tecnologías Fotónicas, Instituto de Investigación en Ingeniería de Aragón (I3A), Universidad de Zaragoza, Zaragoza (Spain)

E-mail: rchueca@unizar.es

Abstract. Perimetrally uncoated windows can be a simple and low cost solution to the problem of radio frequency transmission in low-e glass when the requirements are not too demanding. However, this kind of non-uniform and relatively large structures are difficult to characterize experimentally. The aim of this work is to develop and experimentally verify a method for the simulation of the RF transmission of perimetrally uncoated windows. We propose to study these windows as a composition of four rectangular apertures in a metallic sheet. Using numerical simulations, we are able to obtain the transmission coefficient of these apertures. Then, a multilayer model based on transmission line theory is used to consider the effect of the different glazings and cameras which can be part of a window. Finally, the results of this study are compared to the measurements of complete windows in the 1000 MHz – 6000 MHz frequency range.

Keywords: Radiofrequency, low-e glass, perimetrally, aperture, multilayer

Submitted to: *J. Phys. D: Appl. Phys.*

1. Introduction

Energy-efficient glass is widely used in the architectural and automotive industries. This feature is obtained by the deposition of nanometric layers of different materials, some of them metals, over the glass substrate. Depending on the placement of these coatings, advanced glasses can attenuate infrared light in a hot climate (solar control glass) or prevent thermal losses in cold weather (low emissivity glass) [1, 2]. Metallic coatings, however, also result in an important attenuation (30-40 dB) of the electromagnetic waves in the mobile communication frequency range [3, 4]. This effect can be perceived in some vehicles such as trains where mobile network coverage problems are notorious.

To avoid this issue, it is necessary to find ways to lower the radiofrequency attenuation of these windows to levels compatible with mobile communication networks, while maintaining advanced thermal properties.

One of the usual solutions is the design of Frequency Selective Surfaces (FSS) [5], where a periodic pattern defined on the metallic layer results in structures that selectively let through a range of frequencies. Even though this is a good solution to the attenuation of RF signals, it is quite an expensive solution, and it can have an important visual impact when used in vehicles or buildings [6–12].

Another solution that can be considered to reduce the attenuation of electromagnetic waves in the mobile communications frequency range is the design of perimetrally uncoated glasses. In this case, the metallic layer is removed from the edge of the glass in order to allow for the RF transmission. This is the area with the lowest visual impact, both because of its situation and because it is usually covered by some opaque non metallic protection when inserting the window into its frame. In [13], a preliminary study of these structures is carried out, focused on experimental measurements with a closed metallic chamber around the glass samples.

The main goal of this research is the theoretical and experimental study of perimetrally uncoated glasses in order to develop a simulation model able to predict the RF attenuation of these kind of glasses. These structures are both large compared to the dimensions of the usual measurement systems and non-uniform over their surfaces, making their experimental characterization difficult, so a design technique like this could be very useful.

When the windows are placed in trains, where the structure of the wagon is also metallic, perimetrally uncoated glasses can be studied as composition of rectangular apertures in an infinite conducting plane.

There are four rectangular apertures in our design: two horizontal and two vertical (Figure 1). For simplicity, we will consider that the metallic regions are both perfect conductors. We will study these structures in the 1 to 6 GHz frequency range used for mobile communications.

Table 1: Comparison with other studies

Ref.	Aperture dim. (mm)	Freq. (GHz)	Study
[14]	L = 100 W = 5	0.1-1	Shielding effectiveness
[15]	L = 150 W = 37.5	0.1-1	Shielding effectiveness
[16]	W << λ	0.1-1	RF Threat
[17]	L = 100,200 W = 5,30	0.1-1	Shielding effectiveness
[18]	L = 100,114 W = 5,25.4	0.1-1	Shielding effectiveness
[19]	L = 20-100 W = 20-30	0.1-1.2	Shielding effectiveness
[20]	L = 400 W = 2	0.1-1	Shielding effectiveness
[21]	L = 10 W = 0.3	1-20	Metasurfaces
[22]	W << λ	-	Diffraction
[23]	L = 30 W = 10	4-8	Microstrip fed slot antenna
[24]	L = 20 W = 2	1-12	Power through apertures

There are several studies of apertures in the literature for different frequencies, size ranges or applications (Table 1). However, to our knowledge, none of them covers the wide range of ratios between aperture sizes (from 50 to 800 mm) and frequencies (1-6 GHz) that our work uses. In our case, the wavelength and aperture sizes are comparable, so many well-known approximations cannot be applied.

In addition, a multilayer model will be applied to obtain, from simple slot simulations, the attenuation of the complete multi-glazed windows, which are structures composed of different plane layers of glass and air or another gas.

As stated before, the aim of this study is to be able to predict the performance of a perimetrally uncoated window without needing a real sample for its characterisation.

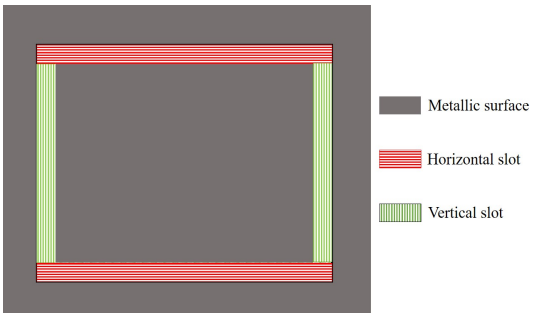

Figure 1: Perimetrally uncoated window and its composition as a structure of four rectangular apertures

2. Theoretical analysis

As a first approach to the problem of the perimetrally uncoated window, we will study horizontal and vertical apertures.

The dimensions of the slot will determine its operating frequency range. We will define l (length) as the dimension normal to the electric field and h (height) as the dimension parallel to it. For simplicity, we assume the electric field from the aperture is parallel to y. Thus, the horizontal slots, perpendicular to the electric field direction, will always have $l > h$, whereas for the vertical slots, parallel to the electric field, $h > l$ (Figure 2).

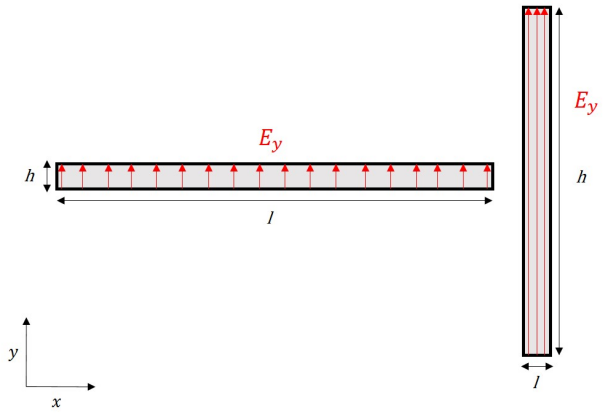

Figure 2: Horizontal and vertical slots excited by a electric field E_y and the dimensions l (length) and h (height)

The electromagnetic wave that reaches a slot generates a difference in electric potential that depends on the height of the slot h and, therefore, the radiated power at a given frequency is proportional to h^2 by a constant k. Therefore, the relationship between the power that reaches the slot (P_0) and the transmitted power $P(h)$ is the following,

$$P(h) = P_0 \cdot k \cdot h^2 \quad (1)$$

This expression is valid in the range where the height of the slot is in the order of the wavelength. Beyond that, the transmitted power is simply proportional to the area of the aperture.

The optimum l for a slot antenna is $\lambda/2$, as its polarization is the opposite of that of a dipole. A slot will then act as a high pass filter and attenuate the frequencies for which l is shorter than $\lambda/2$. For a horizontal slot in a train window, the cutoff frequency of this filter will be under our study range. However, for a vertical slot, l is in the order of a few centimeters, so this frequency will fall squarely in our range of interest.

3. Characterisation of apertures

Our measurement setup (Figure 3) uses two directional Vivaldi antennas (TSA600) working on the 600 to 6000 MHz frequency range, placed in an anechoic chamber.A vector network analyser (picoVNA 106) is used to generate and measure the signals. A metallic sheet is placed around the sample under test to emulate the train coach wall.

Figure 3: Measurement setup for characterisartion of apertures

3.1. Power transmission dependence with the slot dimensions

A series of different apertures has been studied in this setup in order to verify the dependence of the power transmitted power with the dimensions l and h. As stated in the previous section, the electric field polarization used for the measurements is always maintained in the y direction.

Horizontal apertures with height h ranging from 0 to 250 mm have been studied. As expected, the power transmission through a slot for a given frequency is proportional to h^2. Figure 4 shows the

linear relationship between $\sqrt{\frac{P(h)}{P_0}}$ and h for a fixed frequency.

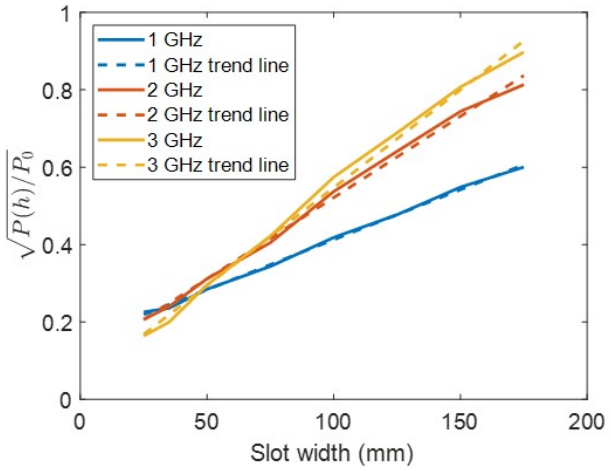

Figure 4: Linear dependence of $\sqrt{P(h)/P_0}$ with h for fixed frequencies

The dependence of the proportionality parameter $\sqrt{k}$ (which is the slope of the lines in Figure 4) with the frequency is also linear, as a change on the wavelength of the signal is equivalent to a change in the dimensions of the aperture (Figure 5).

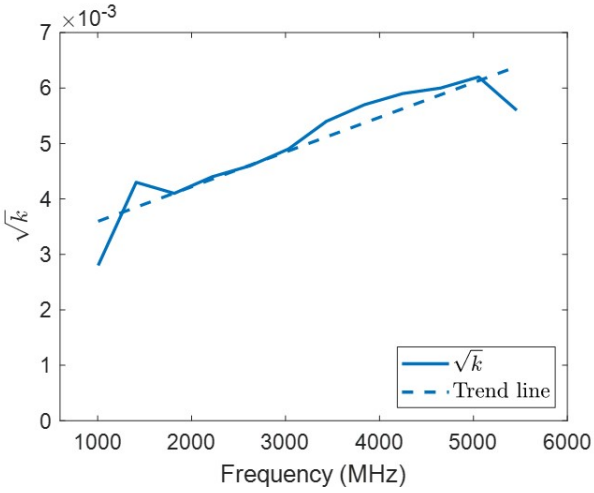

Figure 5: $\sqrt{k(f)}$ coefficient and the linear trend line

We can also make explicit the variation of k with the frequency according to:

$$\sqrt{k(f)} = \alpha f + C = \frac{\alpha c}{\lambda} + C \tag{2}$$

$$P(h) = P_0 \cdot (\alpha f + C)^2 \cdot h^2 \tag{3}$$

The effect of the length l of the aperture has also been studied. For the horizontal slots, the $\lambda/2$ condition is not a problem in the frequency range of the study, as l is larger than λ. The power received through a vertical slot is less than through the equivalent horizontal slot. The reason is that now the dimension l limits the minimum wavelength that goes through the gap. This behaviour can be compared to a high pass filter with a cut-off frequency f_c. Figure 6 shows the measurement results for different values of l, normalized to the maximum for each slot. The cut-off frequencies for the examples are compared on Table 2.

Table 2: Theoretical ($\lambda/2$) and experimental cut-off frequencies (f_c) for different values of l

l (mm)	f_c(GHz) at -3dB	f_c(GHz) at $\lambda/2$
75	2.38	2
50	3.03	3
35	3.948	4.14
25	-	6

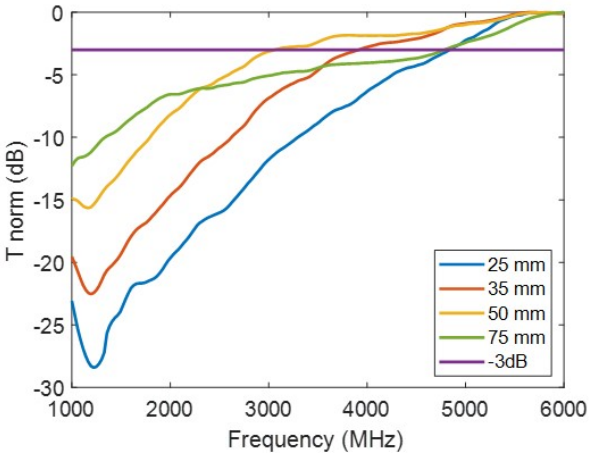

Figure 6: Normalized power transmission in vertical slots for different values of l and cut-off frequencies

3.2. Numerical simulations

After studying the dependence of the power transmitted through the slots with their dimensions, a finite element simulation using COMSOL Multiphysics is performed in order to obtain the transmission coefficient for a perimetrally uncoated window. The values of l and h in these simulations are selected according to the size of a conventional train window (800x636 mm for our samples).

The COMSOL model consists of two air blocks and a perfect electrical conductive surface between them. This contains a rectangular aperture of length l and height h, which will vary in size. The model

is excited by an electromagnetic field with Ey or Hy perpendicular to the slit width, to simulate a horizontal or vertical slit respectively. Perfectly Matched Layers (PML) are added to the model to avoid undesired reflections. This model is evaluated in the frequency domain, from 1 GHz to 6 GHz in steps of 100 MHz.

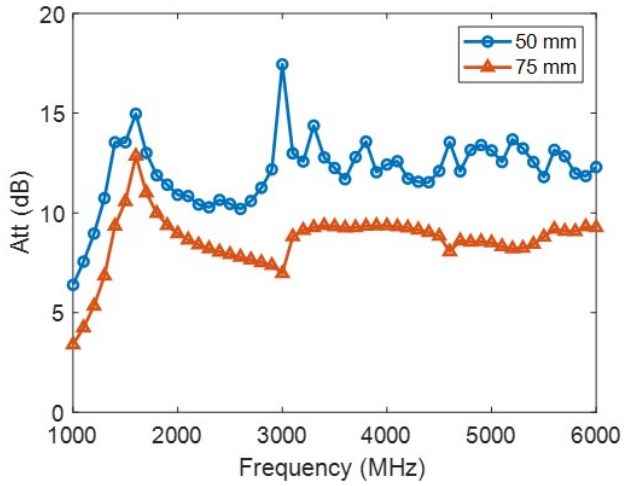

(a)

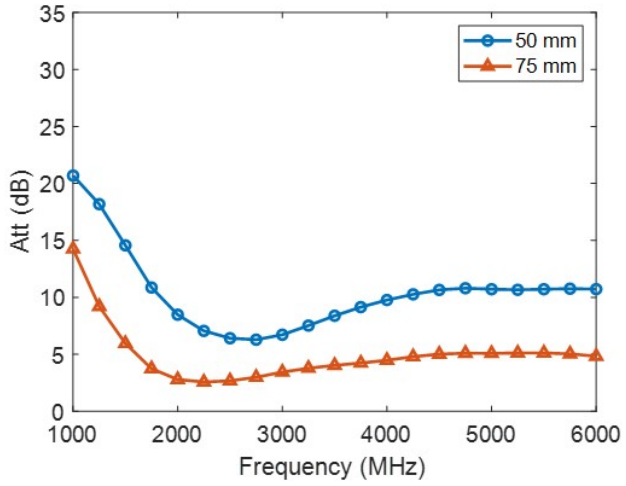

(b)

Figure 7: Simulated attenuation (dB) for horizontal slots with l=800 mm and different h values (a) and for vertical slots with h=800 mm and different l values (b)

In Figure 7a , the simulated attenuation (dB) for horizontal slots of $l = 800mm$ and $h = 50mm$ and $75mm$ are represented. Their shapes are similar, with a minimum at 1 GHz, maxima at 1.5 GHz and more or less constant value for the remaining range. The attenuation is higher for the 50 mm slot, as expected due its smaller h. Figure 7b shows the simulated attenuation (dB) for vertical slots of $h = 800mm$ and $l = 50$ and $75mm$. As it happened with the horizontal slots, both lines follow the same trend but with an offset in attenuation due to the value of l. The maximum is at 1 GHz for both cases and the minimum changes with l as it depends on $\lambda/2$.

Using the results of previous simulations, we can obtain the the S_{21} parameter of the structure ($Att(dB) = -20\log(S_{21})$) and, from it, the equivalent impedance of the slot:

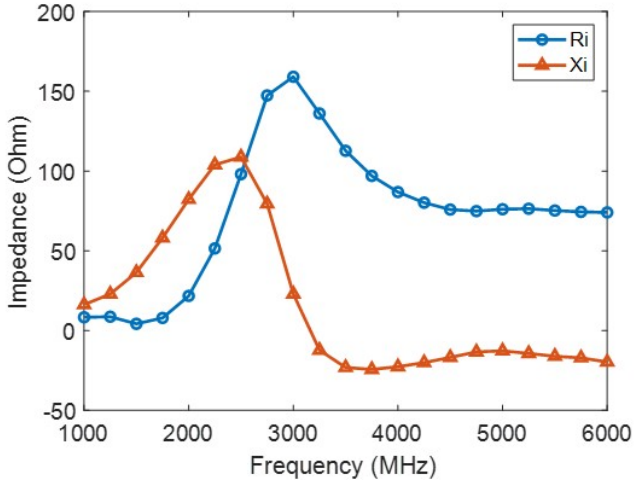

(a)

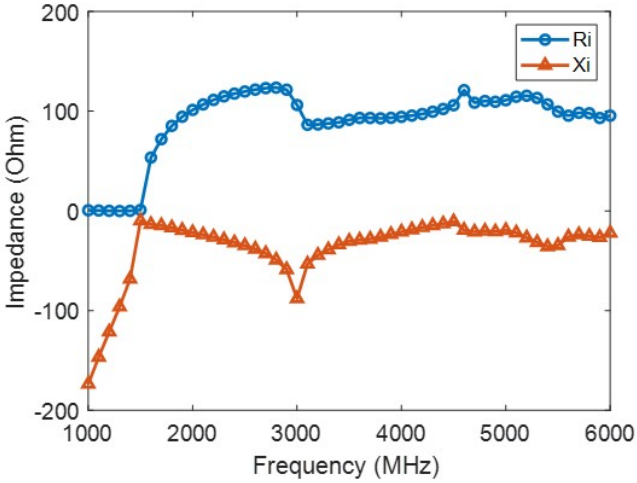

(b)

Figure 8: Equivalent complex impedance of a 50x800mm vertical slot (a) and of a 800x75mm horizontal slot (b)

$$S_{21} = 1 + S_{11} = 1 + \frac{Z_{in} - \eta_0}{Z_{in} + \eta_0} = \frac{2Z_{in}}{Z_{in} + \eta_0} \tag{4}$$

$$Z_{in} = \frac{Z_{slot} - \eta_0}{Z_{slot} + \eta_0} \tag{5}$$

$$Z_{slot} = \frac{-S_{21}\eta_0}{2(S_{21} - 1)} \tag{6}$$

As an example, the real (R_i) and imaginary (X_i) part of the impedance of two different slots are shown: one vertical slot of 50x800 mm (Figure 8a) and one horizontal slot of 800x75 mm (Figure 8b). For the vertical slot, the reactance changes from positive to negative at 3 GHz, when the length $l = \lambda/2$. For the horizontal slot the minimum in resistance and reactance is at 1GHz (as the minimum attenuation). At the maximum of attenuation (1.5 GHz) the resistance increases to 100 Ω and the reactance tends to 0.

Once the equivalent complex impedance of a slot has been calculated, it can be introduced in a transmission line model. This will be necessary to study the multiglazed windows in the next section.

The attenuation of the complete window perimeter can be obtained in two ways. The first approach is to simulate the complete structure, which is a time and resources intensive process. The second is to obtain the total attenuation as a composition of the previous values for the horizontal and vertical slots. This is not only a faster process, but also will be the only available option for the experimental characterization of the windows, as their size makes very difficult a measurement of the complete structure in a conventional setup.

Thus, it is important to verify that the results of the simulations of the window as a whole and as the composition of four slots are similar, so we can then also use a composition of slots for the experimental characterization.

The perimetrally uncoated window is divided in two different structures, as represented in Figure 9, one considering just the horizontal slots and one with vertical slots. Each of these structures can be divided in sections of equal size, containing either the slots (with transmission coefficients T_1 and T_2) or the intermediate area, covered by a metallic layer with a transmission coefficient $T_3 \approx 0$.

The total transmission coefficient of the perimeter is calculated as the sum of the transmission coefficient of two horizontal slots and two vertical slits. $n_{H,V}$ is the number of sections in the horizontal and vertical structures, which depends on the size of the window and the aperture of the antennas used in the measurement or simulation. For example, in a 800x636 mm window using an antenna with 160 mm aperture width, n_H=5.2 and n_V=6.77.

$$T_H = \frac{2T_1}{n_H} \tag{7}$$

$$T_V = \frac{2T_2}{n_V} \tag{8}$$

$$T_T = T_H + T_V \tag{9}$$

$$Att_T(dB) = -10\log(T_T) \tag{10}$$

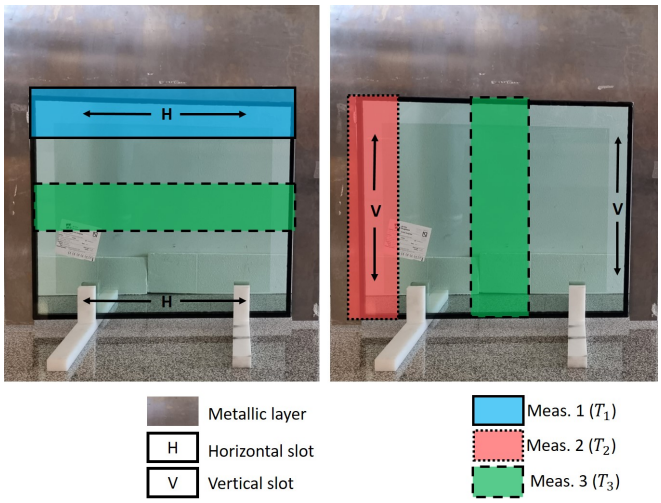

Figure 9: Measurement method to calculate the average transmission T_H with two horizontal slits (left) and the average transmission T_V with two vertical slits (right) in a real sample of 75 mm perimetrally uncoated double glazed window

The comparison between the simulation of the complete structure and the composition of four slots is shown in Figure 10. In this graph it can be seen in blue, the simulation of the complete geometry and, in orange, the composition of the four slots simulated individually, as a structure of 2 horizontal and 2 vertical slots.

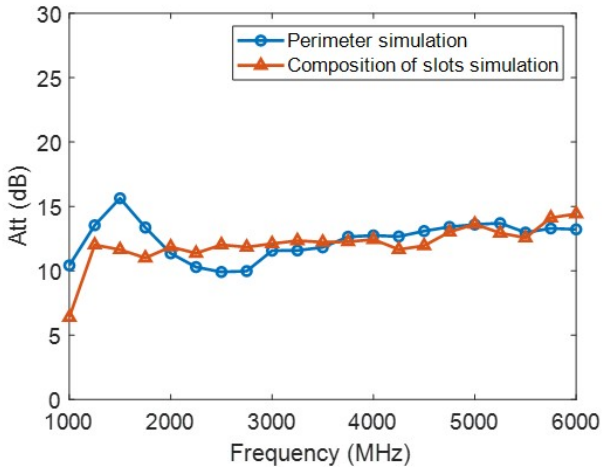

Figure 10: Simulated attenuation of a metallic sheet with an aperture of 50 mm around its perimeter.

4. Multi-glazed windows

Multi-glazed windows are complex structures composed by different materials. These structures can con-

tain multiple glass layers and air or gas chambers of variable size, which affect the electromagnetic transmission performance of the slots, as the thickness of the glazing layers, and especially the spacing cavities, is in the order of the wavelengths involved. This effect will be studied using a transmission line model [25].

In this study, the windows used are 800x636 mm double glazed samples. The glazing is formed by a laminated glass (two 4 mm monolithic glasses separated by 1.5 mm of polyvinyl butyral), an air chamber of 15 mm and a third glass of 5 mm. The metallic low-e layer is on side four, i.e. between the second glass and the air gap.

4.1. Multilayer model

The proposed model considers the window as a multilayer structure with layers of different thicknesses and refractive indices. Each of these layers is equivalent to a section of transmission line of length equal to its thickness.

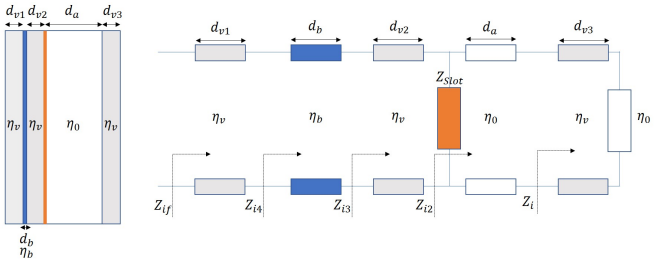

Figure 11: Perimetrally uncoated double glazed window and its equivalent multilayer model

The objective of this model (shown in Figure 11)is to calculate the equivalent input impedance of the structure. To achieve this, and using the expression (11), the intermediate impedances are calculated from right to left using equation (11).The glass impedance (η_V)is assumed to be real (no losses) and equal to η_0/n_V with $n_V = 2.68$.

$$Z_i = R_0 \frac{Z_L + jR_0 \tan \beta l}{R_0 + jZ_L \tan \beta l} \tag{11}$$

In the first step, the load Z_L is the intrinsic impedance of the air η_0 and the line section $l = d_1$ is the last glass layer. The characteristic impedance of the layer of thickness d_1 is η_1 and, therefore,

$$Z_i = \eta_1 \frac{\eta_0 + j\eta_1 \tan \beta l}{\eta_1 + j\eta_0 \tan \beta l} = \eta_1 \frac{\eta_0 + j\eta_1 \tan(\frac{2\pi f \eta_1}{c\eta_0} d_1)}{\eta_1 + j\eta_0 \tan(\frac{2\pi f \eta_1}{c\eta_0} d_1)} \tag{12}$$

Once Z_i is calculated, the process is repeated until the input impedance Z_{if} is obtained. With the value of this final impedance the power transmission coefficient(T) and thus the value of the attenuation (Att) can be calculated.The fraction of the power available at the generator delivered to a transmission line (G_{in}) with an input impedance Z_{if} is

$$G_{in} = \frac{Re(Z_{if})}{4\eta_0 |Z_{if} + \eta_0|^2} \tag{13}$$

In a circuit with lossless lines and no derivations, the power delivered to the input impedance is the same than the power delivered to the load. The fraction of power delivered to the load is the same as the power transmission coefficient of the glazing, so

$$T = G_{in} \tag{14}$$

$$Att(dB) = -10 \log(T) \tag{15}$$

For a perimetrally uncoated window, the only change in the multilayer model is that the impedance of the slot (Z_{Slot})is added in parallel at the corresponding position (in orange in Figure 11). This impedance can be obtained from the COMSOL simulations as shown in the previous section. This will change the input impedance of the circuit. Also, we have to calculate the fraction of the power not derived to the slot.

$$F_{ns} = \frac{Re(\frac{1}{Z_{iS}})}{Re(\frac{1}{Z_{Slot}}) + Re(\frac{1}{Z_{iS}})} \tag{16}$$

Where Z_{iS} is the equivalent impedance prior to the slot. The transmission coefficient of the glazing will now be

$$T = G_{in} \cdot F_{ns} \tag{17}$$

This calculation method has been implemented using Matlab and the impedance Z_{Slot} calculated previously with COMSOL.

4.2. Results

As a first step, this multilayer model has been used to obtain the attenuation of a double glazed window with only one slot in its metallic layer, as shown in Figure 12a and Figure 12b.

The simulated attenuation is then compared to experimental measurements of a real window (Figure 13), but also with only an uncoated slot, instead of the complete perimeter.

The results, shown in Figure 14a and Figure 14b, validate the use of the numerical simulations to calculate the equivalent impedance and compute the attenuation using a multilayer method.

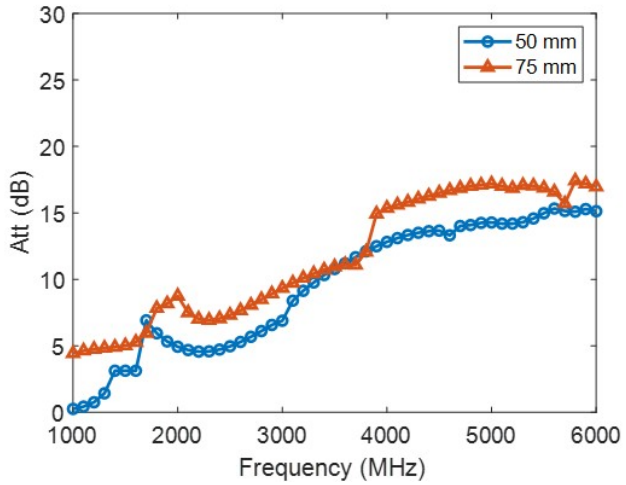

(a)

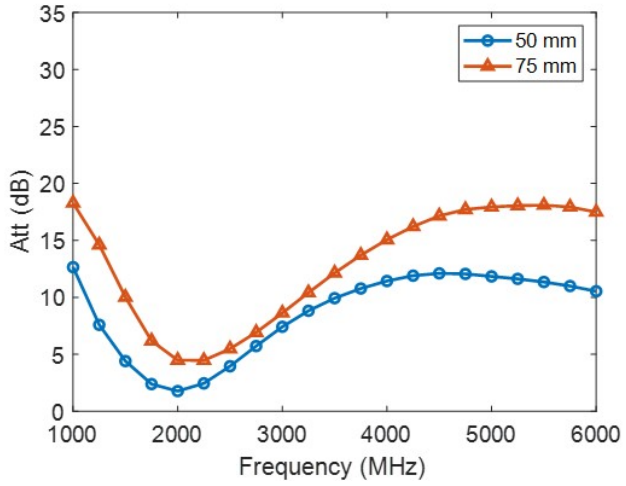

(b)

Figure 12: Simulated attenuation of a double glazed window with one horizontal slot of 50 and 75 mm (a) and with one vertical slot of 50 and 75 mm (b)

Figure 13: Measurement setup for the attenuation of uncoated perimeter windows

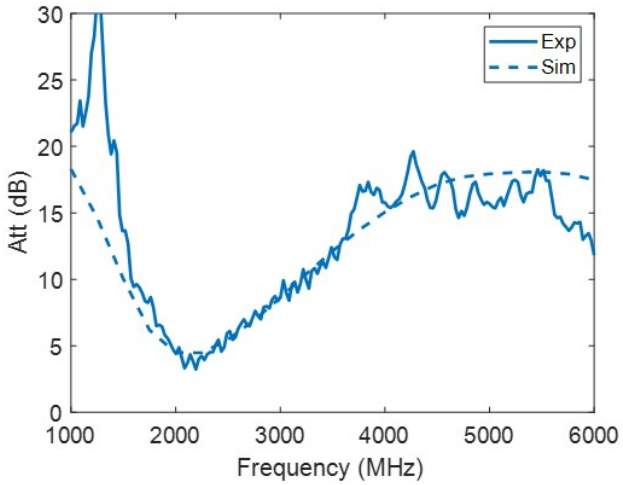

(a)

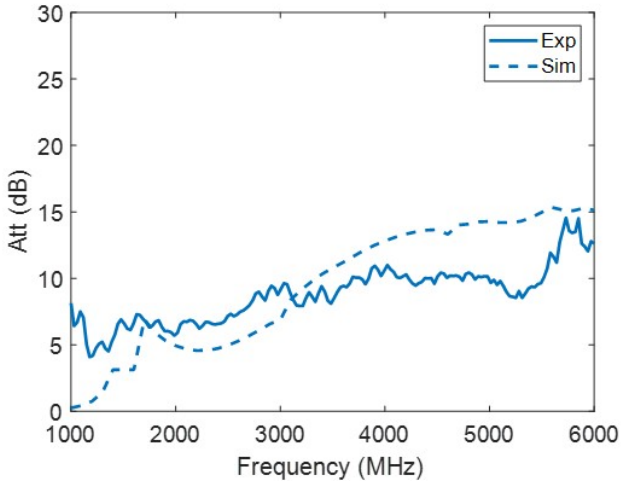

(b)

Figure 14: Simulation and measurement of a double glazed window with one vertical slot of 50x800 mm (a) and of a double glazed window with one horizontal slot of 75x800 mm (b)

As it has been stated in the previous sections, the transmission properties of these windows are not uniform over their surface and, consequently, measuring the global attenuation of these windows is not an easy task. To do this, we use the composition technique described in section 3.2, placing the antennas in three different positions: at the horizontal slot, at the vertical and in the middle of the window where there is no aperture. A reference power measurement to calculate attenuation is also taken at the same positions but without the window.

The transmission coefficient of the complete window can then be calculated as the sum of the transmission coefficient of a glass with two horizontal

slits and a glass with two vertical slits, as previously explained. Figure 15 shows the comparison between the simulated results and the measurements, with good agreement.

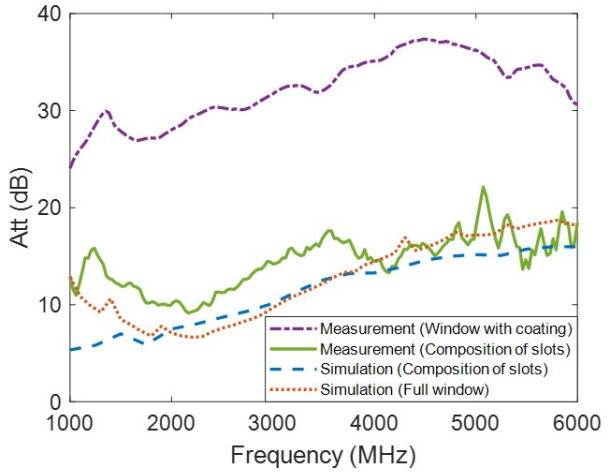

Figure 15: Comparison between simulated and measured attenuation of a complete 50 mm perimetrally uncoated window and a conventional window with metallic coating (low-e glass).

The simulations have been performed using two different methods to obtain the impedance of the metallic layer with COMSOL: a) calculating the impedance of each of the four different slots and using the composition technique or b) computing directly the impedance of the metallic layer with the full uncoated perimeter. Both methods result in similar attenuation values, reinforcing the soundness of our composition technique.

This graph also contains the measurement of a window with metallic coating (low-e window) to show how the attenuation of the window has changed with the perimetrally uncoated solution.

The attenuation of a 50 mm perimetrally uncoated window is between 10 and 15 dB for the frequency range studied. These values are slightly higher than those usually reported for windows using frequency selective surfaces [8]. However, it should be noted that the aim of this work is not to improve over the performance of FSS windows but to provide a simulation and design method for an alternative technique (perimetrally uncoated windows). This technique may be of interest in some situations where its advantages in cost, complexity and visual impact outweigh RF attenuation.

5. Conclusions

This study presents an analysis of perimetrally uncoated glasses as a composition of rectangular apertures. First, the rectangular slot has been studied in order to understand the behaviour of electromagnetic waves in this structure, including power distribution and dependency on size and polarization. Then, a numerical simulation has been used to obtain the attenuation of different apertures and their equivalent impedance.

A composition technique to obtain the total attenuation of a perimetrally uncoated glass from the attenuation of individual slots has been presented. This technique, validated by the simulations, provides also an experimental method to estimate the attenuation in large and non-uniform windows, which can not be measured directly.

The equivalent impedances obtained from the simulations have been introduced in a multilayer model based on transmission lines, in order to predict the attenuation of multi-glazed windows without the need of the measurement of a real sample.

The simulation results have been compared to the measurements of prototypes for commercial windows, showing good agreement. Both the simulation method and the experimental measurement technique are useful tools for the design of perimetrally uncoated windows. These structures can be a simple and non expensive solution to the problem of RF signal attenuation in low-e windows when the attenuation requirements are not very demanding.

Acknowledgments

The authors would like to thank Leyre Tejedor and Ariño Duglass for providing the samples used in this work.

This study has been funded by FEDER/Ministry of Science, Innovation and Universities - State Research Agency (project RTC2019-007368-3)

References

[1] O. Bouvard, M. Lanini, L. Burnier, R. Witte, B. Cuttat, A. Salvade, and A. Schüler, "Structured transparent low emissivity coatings with high microwave transmission," *Applied Physics A*, vol. 123, no. 1, pp. 1–10, 2017.

[2] A. Karttunen, M. Mökkönenn, and K. Haneda, "Investigation of 5g radio frequency signal glazing structures," *Glass Perfomance Days*, 2019.

[3] P. Ängskog, M. Bäckström, and B. Vallhagen, "Measurement of radio signal propagation through window panes and energy saving windows," in *2015 IEEE international symposium on electromagnetic compatibility (EMC)*, pp. 74–79, IEEE, 2015.

[4] P. Ragulis, P. Ängskog, R. Simniškis, B. Vallhagen, M. Bäckström, and Ž. Kancleris, "Shielding effectiveness of modern energy-saving glasses and windows," *IEEE*

Transactions on Antennas and Propagation, vol. 65, no. 8, pp. 4250–4258, 2017.

[5] B. A. Munk, *Frequency selective surfaces: theory and design*. John Wiley & Sons, 2005.

[6] G. I. Kiani, A. Karlsson, L. Olsson, and K. P. Esselle, "Glass characterization for designing frequency selective surfaces to improve transmission through energy saving glass windows," in *2007 Asia-Pacific Microwave Conference*, pp. 1–4, IEEE, 2007.

[7] O. Danila, "Polyvinylidene fluoride-based metasurface for high-quality active switching and spectrum shaping in the terahertz g-band," *Polymers*, vol. 13, no. 11, p. 1860, 2021.

[8] L. Burnier, M. Lanini, O. Bouvard, D. Scanferla, A. Varathan, C. Genoud, A. Marguerit, B. Cuttat, N. Dury, R. Witte, *et al.*, "Energy saving glazing with a wide band-pass fss allowing mobile communication: up-scaling and characterisation," *IET Microwaves, Antennas & Propagation*, vol. 11, no. 10, pp. 1449–1455, 2017.

[9] G. I. Kiani, L. G. Olsson, A. Karlsson, K. P. Esselle, and M. Nilsson, "Cross-dipole bandpass frequency selective surface for energy-saving glass used in buildings," *IEEE Transactions on Antennas and Propagation*, vol. 59, no. 2, pp. 520–525, 2010.

[10] M. Gustafsson, A. Karlsson, A. P. P. Rebelo, and B. Widenberg, "Design of frequency selective windows for improved indoor outdoor communication," *IEEE transactions on antennas and propagation*, vol. 54, no. 6, pp. 1897–1900, 2006.

[11] A. A. Dewani, S. G. O'Keefe, D. V. Thiel, and A. Galehdar, "Window rf shielding film using printed fss," *IEEE Transactions on antennas and propagation*, vol. 66, no. 2, pp. 790–796, 2017.

[12] R. Alcain, E. Carretero, R. Chueca, C. Heras, and I. Salinas, "Study of optical, thermal and radio frequency properties of low emissivity coatings with frequency selective surfaces," *Journal of Physics D: Applied Physics*, vol. 55, no. 6, p. 065502, 2021.

[13] R. Chueca, R. Alcain, C. Heras, and I. Salinas, "Closed metal chamber configuration for estimating rf attenuation in vehicles with advanced thermal properties windows," in *2022 16th European Conference on Antennas and Propagation (EuCAP)*, pp. 01–04, IEEE, 2022.

[14] G. Wu, Z.-Q. Song, X.-G. Zhang, and B. Liu, "Study on coupling characteristics of electromagnetic wave penetrating metallic enclosure with rectangular aperture," *The Applied Computational Electromagnetics Society Journal (ACES)*, pp. 611–618, 2011.

[15] I. B. Basyigit, H. Dogan, and S. Helhel, "The effect of aperture shape, angle of incidence and polarization on shielding effectiveness of metallic enclosures," *Journal of Microwave Power and Electromagnetic Energy*, vol. 53, no. 2, pp. 115–127, 2019.

[16] J. J. Lemmon, *Analysis of the RF Threat to Telecommunications Switching Stations and Cellular Base Stations*, vol. 2. US Department of Commerce, National Telecommunications and Information , 2002.

[17] M. P. Robinson, T. M. Benson, C. Christopoulos, J. F. Dawson, M. Ganley, A. Marvin, S. Porter, and D. W. Thomas, "Analytical formulation for the shielding effectiveness of enclosures with apertures," *IEEE transactions on Electromagnetic Compatibility*, vol. 40, no. 3, pp. 240–248, 1998.

[18] H. Li and P. Amleshi, "An estimate of plane wave leakage through a rectangular aperture," in *2018 IEEE Symposium on Electromagnetic Compatibility, Signal Integrity and Power Integrity (EMC, SI & PI)*, pp. 36–40, IEEE, 2018.

[19] C. H. Kraft, "Modeling leakage through finite apertures with tlm," in *Proceedings of IEEE Symposium on Electromagnetic Compatibility*, pp. 73–76, IEEE, 1994.

[20] F. Olyslager, E. Laermans, D. De Zutter, S. Criel, R. De Smedt, N. Lietaert, and A. De Clercq, "Numerical and experimental study of the shielding effectiveness of a metallic enclosure," *IEEE transactions on Electromagnetic Compatibility*, vol. 41, no. 3, pp. 202–213, 1999.

[21] S. S. Bukhari, W. G. Whittow, J. Vardaxoglou, and S. Maci, "Equivalent circuit model for coupled complementary metasurfaces," *IEEE Transactions on Antennas and Propagation*, vol. 66, no. 10, pp. 5308–5317, 2018.

[22] M. Suzuki, "Diffraction of plane electromagnetic waves by a rectangular aperture," *IRE Transactions on Antennas and Propagation*, vol. 4, no. 2, pp. 149–156, 1956.

[23] B. Zheng and Z. Shen, "Effect of a finite ground plane on microstrip-fed cavity-backed slot antennas," *IEEE transactions on antennas and propagation*, vol. 53, no. 2, pp. 862–865, 2005.

[24] O. M. Ramahi and L. Li, "Analysis and reduction of electromagnetic field leakage through loaded apertures: A numerical study," *Electromagnetics*, vol. 25, no. 7-8, pp. 679–693, 2005.

[25] J. R. Wait, *Electromagnetic waves in stratified media: Revised edition including supplemented material*, vol. 3. Elsevier, 2013.